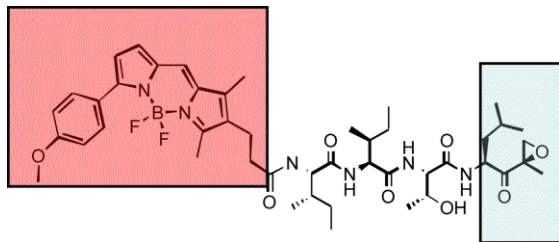


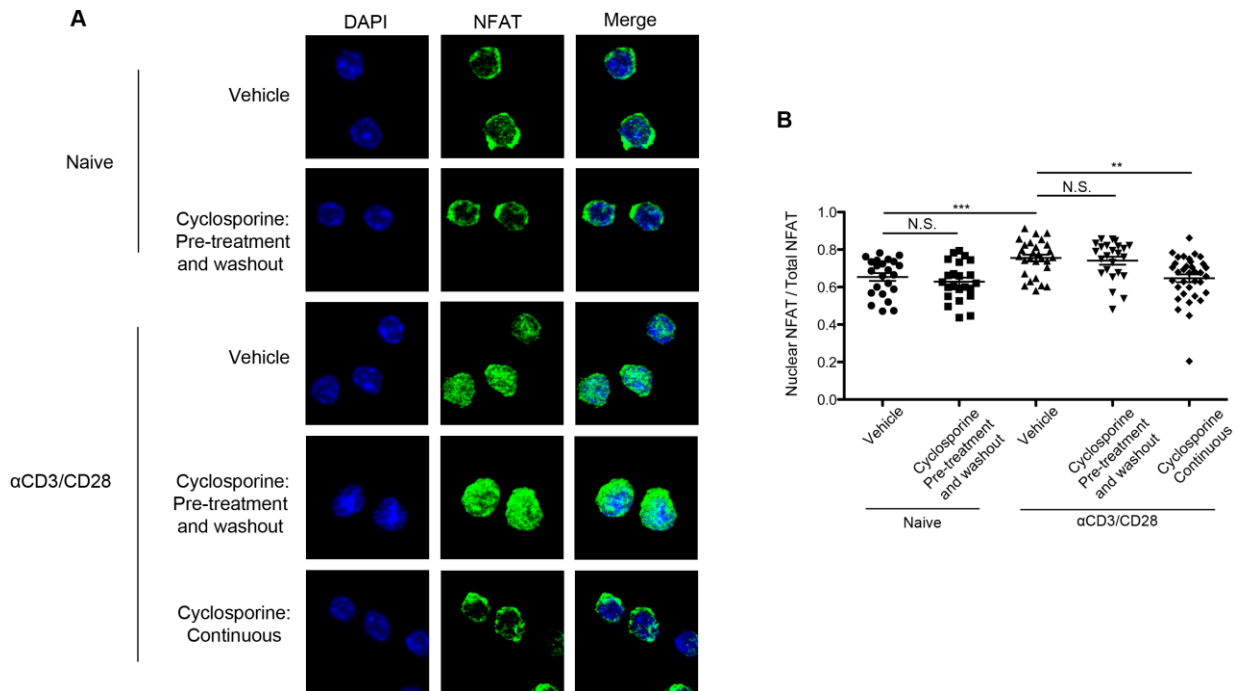
## Supplemental Data



### Supplemental Figure 1. Structure of the pan-reactive proteasome probe MV003.

Highlighted in blue is the epoxyketone warhead and in red is a BODIPY TMR fluorochrome.

MV003 has been previously described (1-3).

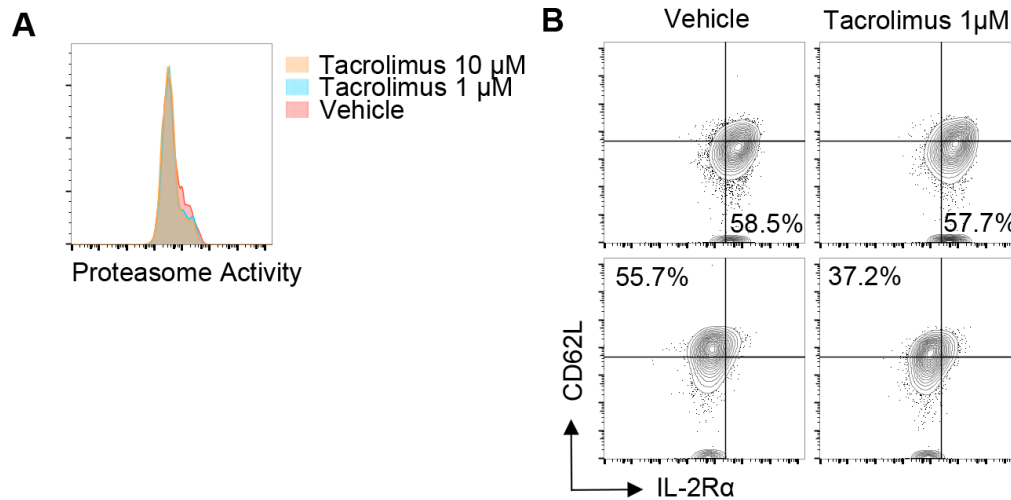


**Supplemental Figure 2. Transient pre-treatment of CD8<sup>+</sup> T cells with cyclosporine followed by drug washout does not block NFAT nuclear translocation.**

Immunofluorescence staining of NFAT (green) in naïve CD8<sup>+</sup> T cells or CD8<sup>+</sup> T cells that were activated *in vitro* with 10 µg/ml immobilized anti-CD3 and anti-CD28 mAbs for 10 minutes.

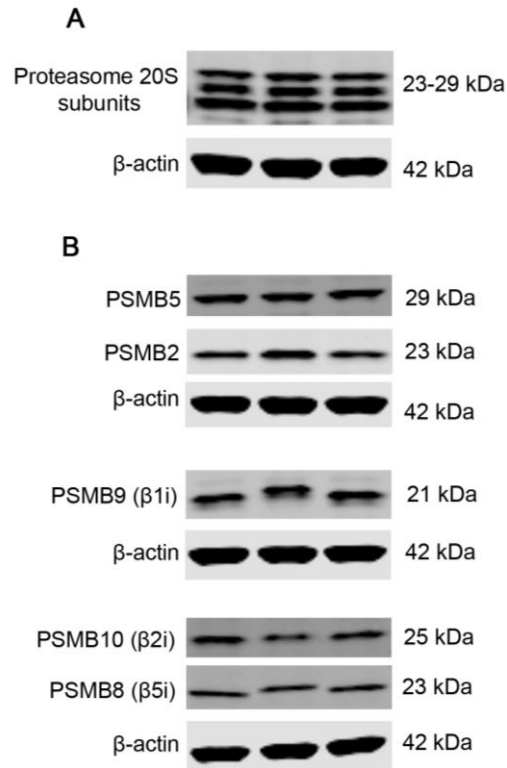
Prior to imaging, naïve CD8<sup>+</sup> T cells were treated for 4 h with DMSO (n = 23) or cyclosporine (n = 23). Prior to imaging, activated CD8<sup>+</sup> T cells were pre-treated with DMSO (n = 27) for 4 h; pre-treated for 4 h with cyclosporine followed by drug washout (n = 35); or pre-treated for 4 h with cyclosporine without drug washout during activation (n = 23) (‘continuous cyclosporine’).

Nuclei were stained with DAPI (blue). Nuclear localization was measured by the ratio of nuclear NFAT over total NFAT. Quantification was performed using NIH ImageJ software. Error bars represent S.E.M., \* p < 0.05, \*\* p < 0.01, \*\*\* p < 0.001 (Student’s t-test).

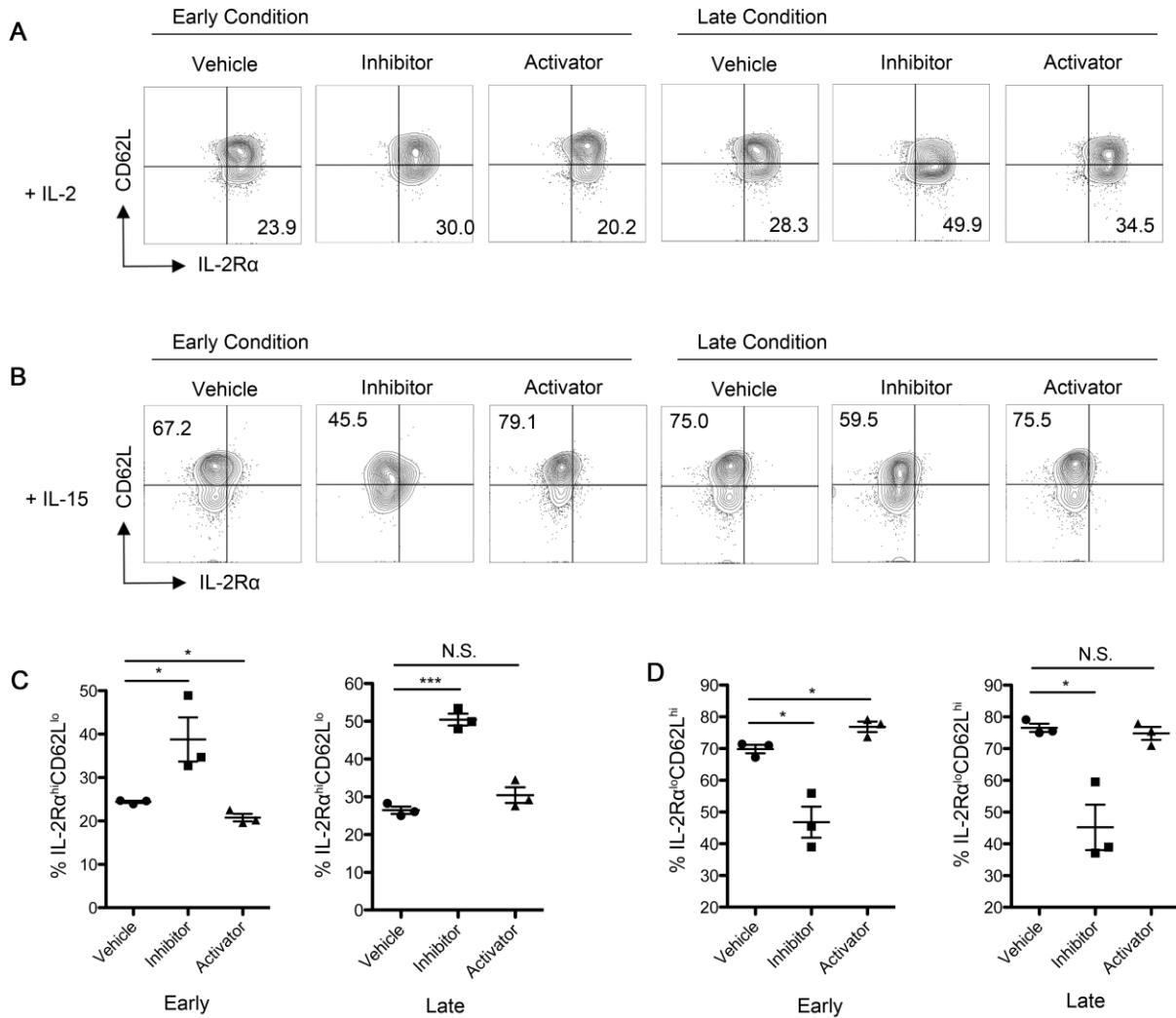


**Supplemental Figure 3. Effects on proteasome activity and CD8<sup>+</sup> T cell differentiation are not a general feature of calcineurin inhibitors.**

(A) Proteasome activity, assessed by flow cytometry, of naïve CD8<sup>+</sup> T cells following 4 h culture with vehicle (red) or the calcineurin inhibitor tacrolimus at 1  $\mu\text{M}$  (blue) and 10  $\mu\text{M}$  (yellow). (B) Flow cytometry analysis of *in vitro* IL-2R $\alpha$ <sup>hi</sup>CD62L<sup>lo</sup> ‘effector-like’ and IL-2R $\alpha$ <sup>lo</sup>CD62L<sup>hi</sup> ‘memory-like’ P14 CD8<sup>+</sup> T cells. Cells were activated for 2 d with gp33-41 peptide and T-depleted splenocytes, then cultured in IL-2 (top row) or IL-15 (bottom row) conditions in the presence of vehicle or tacrolimus. Data are representative of at least two independent experiments (A, B).

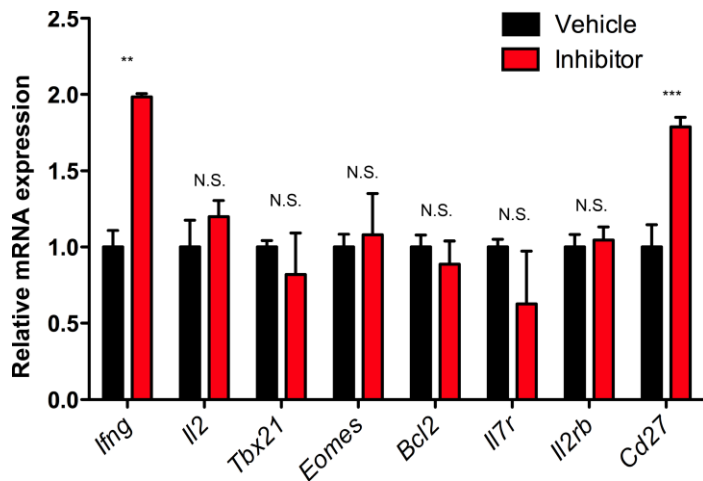


**Supplemental Figure 4. Pharmacological modulation of proteasome activity does not affect 20S proteasome subunit composition.** Expression of structural subunits (A) and catalytic subunits (B) of activated CD8<sup>+</sup> T cells treated with vehicle, proteasome inhibitor, or proteasome activator. Actin was used as loading control. Blots are representative of two independent experiments.

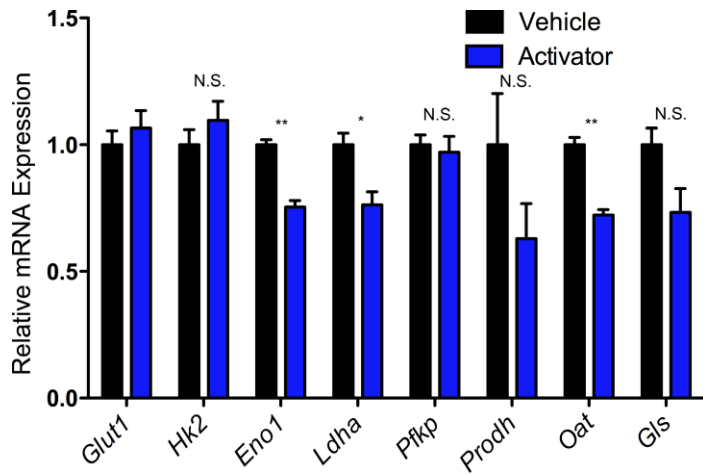


**Supplemental Figure 5. Proteasome inhibitor and activator exhibit distinct effects in early vs. late phases of differentiation *in vitro*.** Analysis of IL-2R $\alpha$  and CD62L expression in CD8 $^+$  T cells activated for 2 d followed by culture in IL-2 (A) or IL-15 (B) along with vehicle, proteasome inhibitor, or proteasome activator (“early condition”) or 2 d after cytokine addition (“late condition”). (C) Quantitation of the proportions of IL-2R $\alpha^{\text{hi}}$ CD62L $^{\text{lo}}$  effector-like cells in early (left) and late (right) differentiation conditions (IL-2 culture). (D) Quantitation of IL-2R $\alpha^{\text{lo}}$ CD62L $^{\text{hi}}$  memory-like cells in early (left) and late (right) differentiation conditions (IL-15

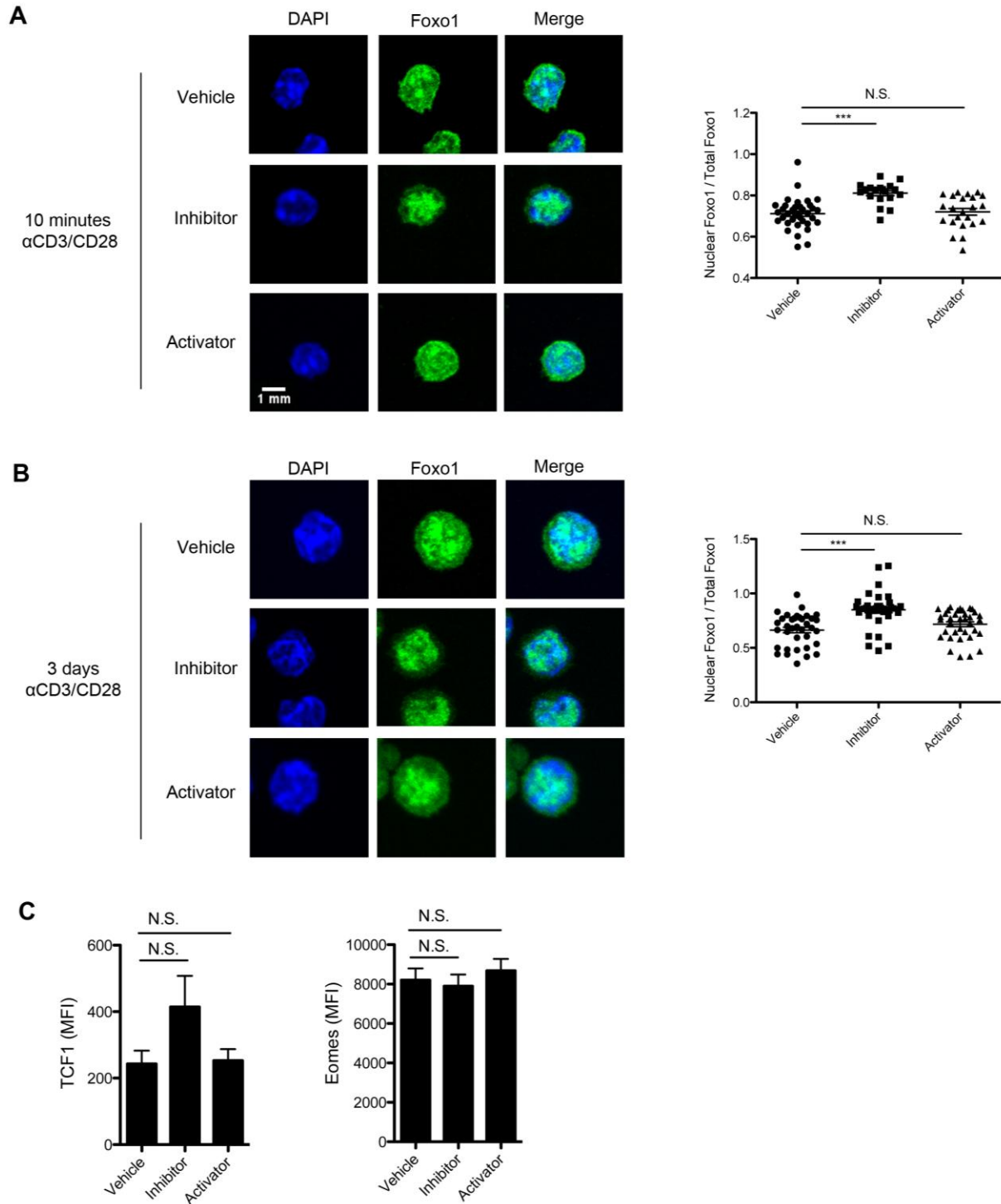
culture).  $n = 3$  from 3 independent experiments. All error bars represent S.E.M. Student's t-test was performed for statistical significance. \*  $p = 0.05$  \*\*  $p = 0.01$  \*\*\*  $p = 0.001$ .



**Supplemental Figure 6. mRNA expression of cytokine genes, effector T cell-associated genes, and memory T cell-associated genes in CD8<sup>+</sup> T cells with decreased proteasome activity.** CD8<sup>+</sup> T cells were treated with DMSO vehicle or proteasome inhibitor, then cultured for 3 days *in vitro* on immobilized antibodies against CD3 and CD28 in the presence of IL-2. RNA was isolated followed by cDNA synthesis for quantitative RT-PCR analysis. n = 3 from 3 independent experiments. All error bars represent S.E.M. Student's t-test was performed for statistical significance. \* p = 0.05 \*\* p = 0.01 \*\*\* p = 0.001.



**Supplemental Figure 7. mRNA expression of glycolysis pathway genes in CD8<sup>+</sup> T cells with increased proteasome activity.** CD8<sup>+</sup> T cells were treated with vehicle or proteasome activator, then cultured for 3 days *in vitro* on immobilized antibodies against CD3 and CD28 with IL-2-containing media. RNA was isolated and cDNA was synthesized for quantitative RT-PCR analysis. n = 3 from 3 independent experiments. All error bars represent S.E.M. Student's t-test was performed for statistical significance. \* p = 0.05 \*\* p = 0.01 \*\*\* p = 0.001.

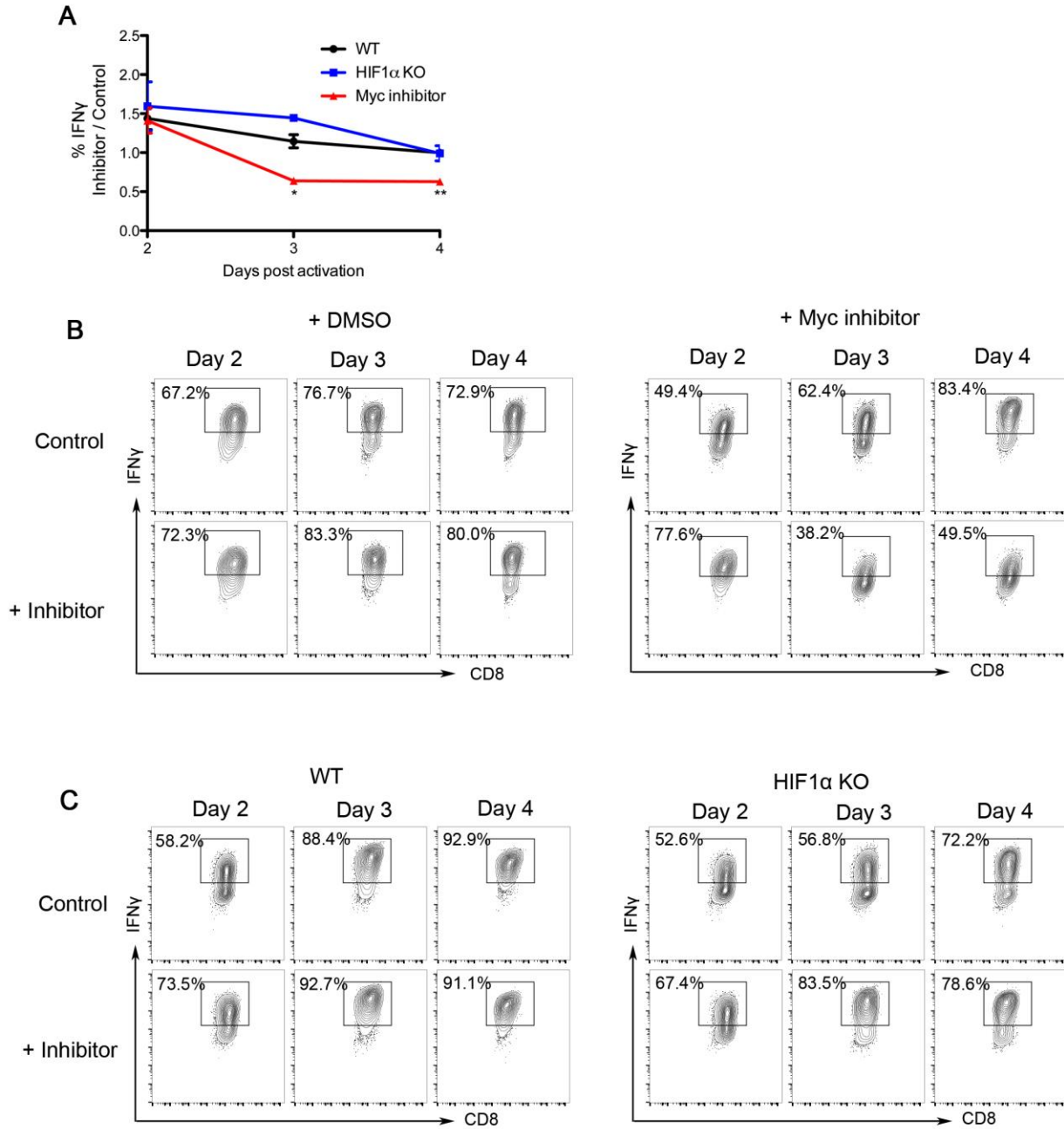


**Supplemental Figure 8. Proteasome modulation does not influence CD8<sup>+</sup> T cell**

**differentiation through nuclear translocation of Foxo1.** (A) Immunofluorescence microscopy

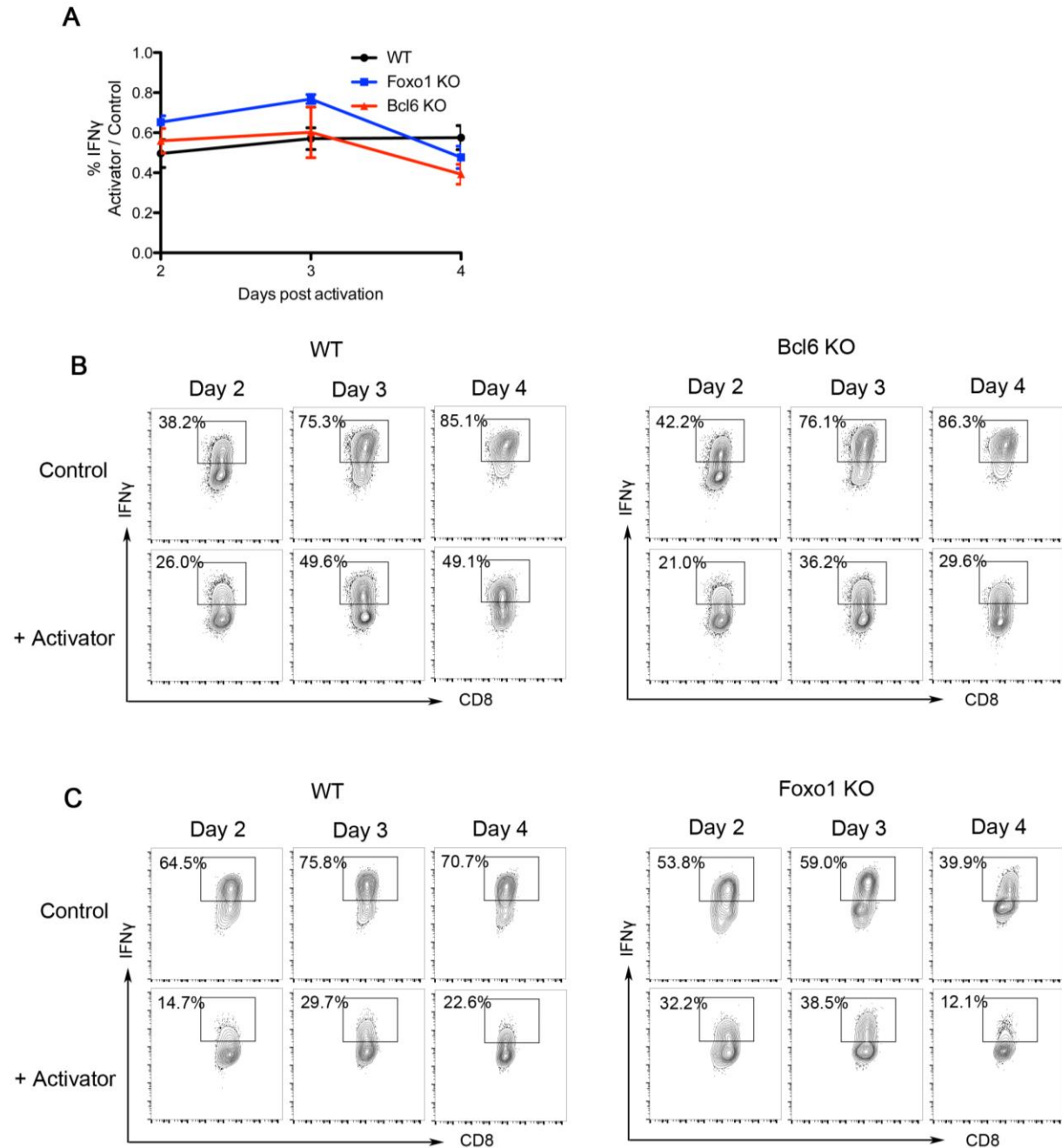
of Foxo1 (green) in CD8<sup>+</sup> T cells pre-treated with vehicle (n = 26), proteasome inhibitor (n =

20), or proteasome activator (n = 19), then activated *in vitro* with immobilized anti-CD3 and anti-CD28 mAbs for 10 m. Nuclei were stained with DAPI (blue). (B) Analysis of Foxo1 nuclear localization of CD8<sup>+</sup> T cells pre-treated with vehicle (n = 36), proteasome inhibitor (n = 39), or proteasome activator (n = 36), then activated *in vitro* with immobilized anti-CD3 and anti-CD28 mAbs for 3 d. Nuclear localization was measured by quantifying the ratio of nuclear Foxo1 relative to total Foxo1. Quantification was performed using NIH ImageJ software. (C) Expression of TCF1 and Eomes (MFI), assessed by flow cytometry, in CD8<sup>+</sup> T cells pre-treated with vehicle, proteasome inhibitor, or proteasome activator, then activated with immobilized anti-CD3 and anti-CD28 mAbs for 3 d. Data are representative of 3 independent experiments. Error bars represent S.E.M., \* p < 0.05, \*\* p < 0.01, \*\*\* p < 0.001 (Student's t-test).



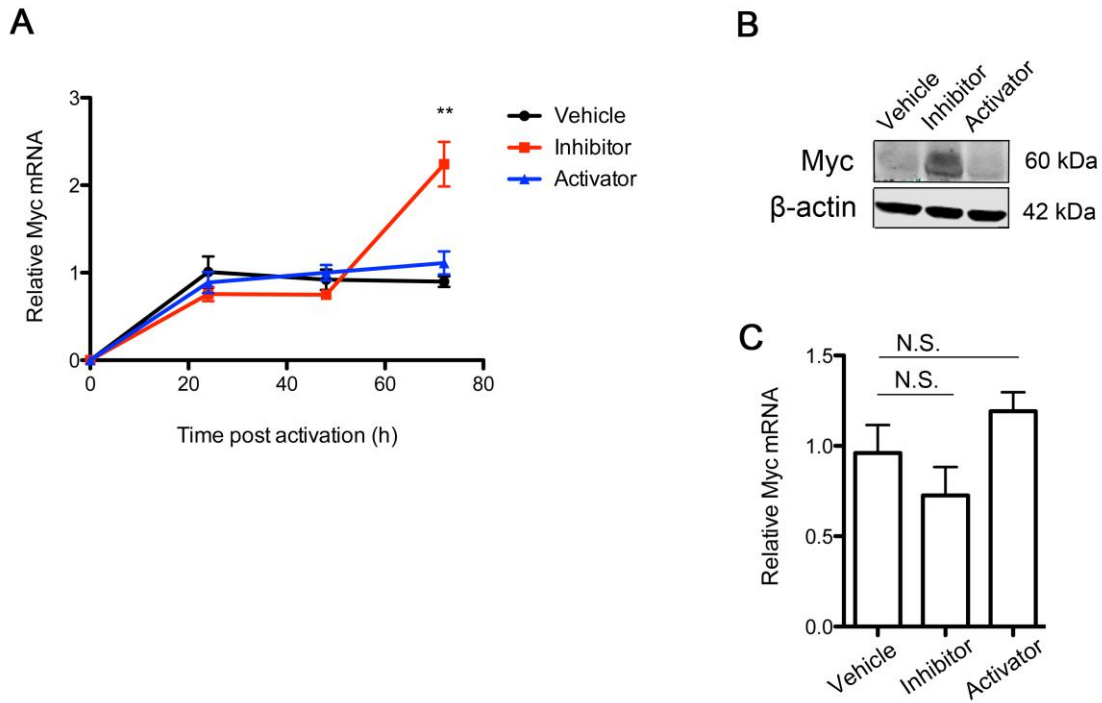
**Supplemental Figure 9. Increased cytokine production induced by proteasome inhibition is dependent on Myc.** (A) Relative IFN $\gamma$  production at 2, 3, or 4 days post-activation by CD8<sup>+</sup> T cells transiently treated with proteasome inhibitor prior to activation followed by addition of DMSO or Myc inhibitor at 24 h post-activation (red line), HIF1 $\alpha$ -deficient CD8<sup>+</sup> T cells (blue

line), or wild-type control cells (black). Data are quantitated as % IFN $\gamma$ <sup>+</sup> in proteasome inhibitor / control. (B) Representative flow cytometry plots of IFN $\gamma$  production in CD8<sup>+</sup> T cells treated with DMSO (left) or Myc inhibitor (right). (C) Representative flow cytometry plots of IFN $\gamma$  production in wild-type (left) or HIF1 $\alpha$ -deficient CD8<sup>+</sup> T cells (right). Data are representative of 3 independent experiments. Error bars represent S.E.M., \*  $p < 0.05$ , \*\*  $p < 0.01$ , \*\*\*  $p < 0.001$  (Student's t-test).

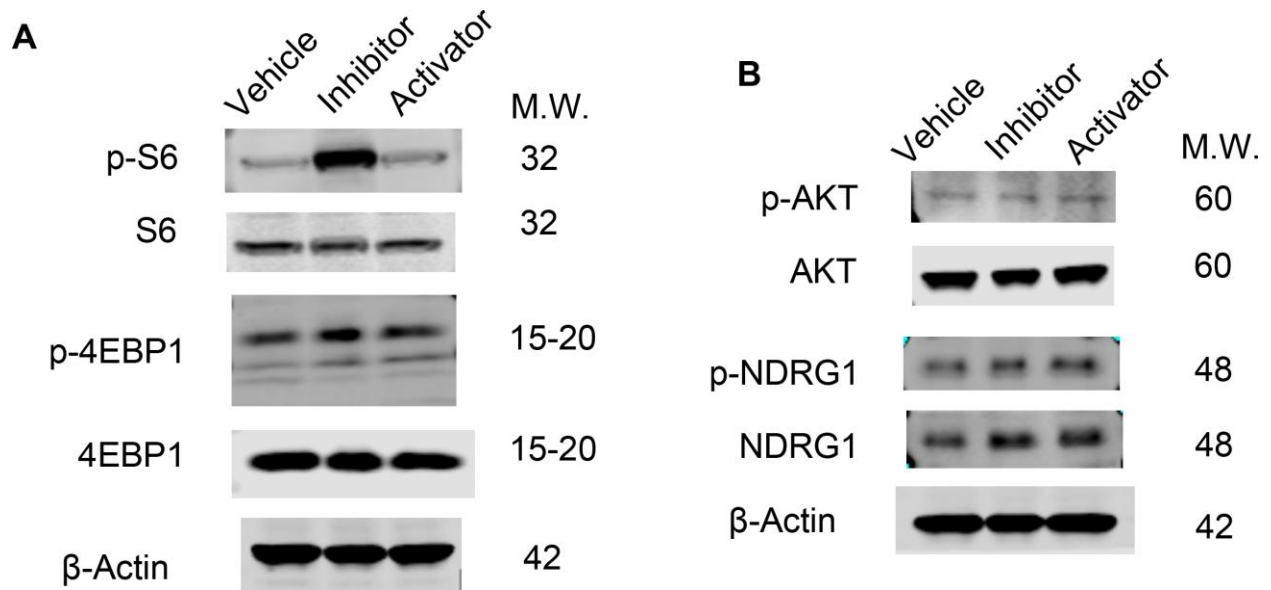


**Supplemental Figure 10. Suppression of cytokine production induced by proteasome activator is not dependent on Foxo1 or Bcl6.** (A) IFN $\gamma$  production at 2, 3, or 4 days by CD8 $^+$  T cells transiently treated with proteasome activator prior to activation. Bcl6-deficient CD8 $^+$  T cells (red line), Foxo1-deficient CD8 $^+$  T cells (blue line), or wild-type control cells (black), post-activation, are quantitated as % IFN $\gamma$  $^+$  in proteasome activator / control. (B) Representative flow

cytometry plots of IFN $\gamma$  production in wild-type (left) or Bcl6-deficient CD8<sup>+</sup> T cells (right). (C)  
Representative flow cytometry plots of IFN $\gamma$  production in wild-type (left) or Foxo1-deficient  
CD8<sup>+</sup> T cells (right). Data are representative of 3 independent experiments. Error bars represent  
S.E.M., \*  $p < 0.05$ , \*\*  $p < 0.01$ , \*\*\*  $p < 0.001$  (Student's t-test).



**Supplemental Figure 11. Proteasome modulation regulates Myc initially through protein degradation.** (A) Relative expression of Myc mRNA in CD8<sup>+</sup> T cells, pre-treated with vehicle, proteasome inhibitor, or proteasome activator, then activated with immobilized antibodies against CD3 and CD28 for 24, 48, or 72 h. (B) Immunoblot analysis of CD8<sup>+</sup> T cells activated with immobilized antibodies against CD3 and CD28 for 24 h followed by treatment with vehicle, proteasome inhibitor, or proteasome activator for 4 h. Actin was used as a loading control. (C) Relative expression of Myc mRNA in activated CD8<sup>+</sup> T cells treated with vehicle, proteasome inhibitor, or proteasome activator, as in B. (A, C) n = 3 from 2 independent experiments. All error bars represent S.E.M. Student's t-test was performed for statistical significance. \* p = 0.05 \*\* p = 0.01 \*\*\* p = 0.001. (B) Representative of 2 independent experiments.



**Supplemental Figure 12. Proteasome inhibition results in increased activation of mTORC1 downstream targets.** (A) Immunoblot analysis of mTORC1 targets, S6 kinase phosphorylation at Ser235/236 and 4EBP1 phosphorylation at Thr37/46, in CD8<sup>+</sup> T cells pre-treated with vehicle, proteasome inhibitor, or proteasome activator followed by activation for 3 days on immobilized anti-CD3 and anti-CD28 mAbs. (B) Immunoblot analysis of mTORC2 targets, Akt phosphorylation at Ser473 and NDRG1 phosphorylation at Thr346, in CD8<sup>+</sup> T cells treated with vehicle, proteasome inhibitor, or proteasome activator followed by activation for 3 days on immobilized anti-CD3 and anti-CD28 mAbs. β-Actin was used as a loading control. Data are representative of 3 independent experiments.

**Supplemental Table 1. Gene lists used for Gene Set Enrichment Analysis (GSEA)**

	MSigDB lists
Genes with increased expression in effector CD8 <sup>+</sup> T cells compared to naïve and memory	GSE1000002_1582_200_UP, GSE1000002_1580_200_DN
Genes with increased expression in naïve CD8 <sup>+</sup> T cells compared to effector and memory	GSE1000002_1580_200_UP, GSE1000002_1581_200_UP
Genes with increased expression in memory CD8 <sup>+</sup> T cells compared to effector and naïve	GSE1000002_1581_200_DN, GSE1000002_1582_200_DN

**Supplemental Table 2. Quantitative Real-Time PCR primers**

	F primer, 5' to 3'	R primer, 5' to 3'
<i>Tbx21</i>	AGCAAGGACGGCGAATGTT	GTGGACATATAAGCGGTTCCC
<i>Gzmb</i>	CCACTCTCGACCCTACATGG	GGCCCCAAAGTGACATTTATT
<i>Il7r</i>	AGTCCTCCTATGTGAGTCCT	ACCCATCTTCTTTGTGTTTCTG
<i>Tcf7</i>	AGCTTTCTCCACTCTACGAACA	AATCCAGAGAGATCGGGGGTC
<i>Ifng</i>	GAGCCAGATTATCTCTTTCTACC	GTTGTTGACCTCAAACCTTGG
<i>Il2</i>	AGCAGCTGTTGATGGACCTA	CGCAGAGGTCCAAGTTCAT
<i>Eomes</i>	TGAATGAACCTTCCAAGACTCAGA	GGCTTGAGGCAAAGTGTTGACA
<i>Bcl2</i>	TCGCAGAGATGTCCAGTCAG	CCTGAAGAGTTCCTCCACCA
<i>Il2rb</i>	CCTTTGACAACCTTCGCCTG	TCTGCTTGAGGCTTAATACGGAT
<i>Cd27</i>	CAGCTTCCCAACTCGACTGTC	GCACCCAGGACGAAGATAAGAA
<i>Glut1</i>	CAGTTCGGCTATAACACTGGTG	GCCCCGACAGAGAAGATG
<i>Hk2</i>	TGATCGCCTGCTTATTCACGG	TGATCGCCTGCTTATTCACGG
<i>Eno1</i>	GGAAAGGAAGACAGAGTGGGAGGC	CAGATCGACCTCAACAGTGGGATTC
<i>Ldha</i>	AAACCGAGTAATTGGAAGTGTTG	TCTGGGTTAAGAGACTTCAGGGAG
<i>Pfkp</i>	GGTACAGATTCAGCCCTGCACC	GTCGGCACCGCAAGTCAAGG
<i>Prodh</i>	GCACCACGAGCAGTTGTTT	CTTTGTTGTGCCGGATCAGAG
<i>Oat</i>	GGAGTCCACACCTCAGTCG	CCACATCCCACATATAAATGCCT
<i>Gls</i>	GTGAATCAGCAAGTGTGATGGC	CCCCCAGCAACTCCAGATTTTG
<i>Rpl13</i>	AGGGCAGGTTCTGGTATTGGAT	AGGCTCGGAAATGGTAGGGG
<i>18S rRNA</i>	GTAACCCGTTGAACCCCAT	CCATCCAATCGGTAGTAGCG

## Supplemental Methods

### *Additional antibodies*

Additional immunoblotting antibodies used were: Proteasome 20S core subunits (Enzo, PW8155), PSMB5 (Abcam, ab3330), PSMB2 (Abcam, ab166628), PSMB9 (Abcam, ab3328), PSMB10 (Abcam, ab183506), PSMB8 (Abcam, ab3329), Foxo1 (Cell Signaling, C29H4), S6 phospho Ser 235/236 (Cell Signaling D57.2.2E), S6 (Cell Signaling 54D2), 4EBP1 phospho Thr37/46 (Cell Signaling 236B4), 4EBP1 (53H11), Akt phospho Ser473 (Cell Signaling 9271), Akt (Cell Signaling C67E7), NDRG1 phospho Thr346 (Cell Signaling, D98G11), NDRG1 (Cell Signaling D8G9).

### *Microarray data processing and gene set enrichment analysis (GSEA)*

Array data was loaded into the Array Studio analysis suite (Omicsoft, Inc.) to perform data visualization and management of analyzed datasets on the cloud. Data was normalized at the gene level and log-transformed before computing one-way ANOVA statistics between treatment and control groups (inhibitor vs. vehicle and activator vs. vehicle). Samples were quality-controlled using principal component analysis to detect possible outliers and batch effects across samples. Differentially expressed gene signatures representing 1-5% of the coding transcriptomes were generated using a log<sub>2</sub> (fold change) value > 1 and a raw p-value of < 0.01. Functional enrichment of differentially expressed genes was performed using the ToppGene Suite (4) and WebGestalt (5). Gene Set Enrichment Analysis (6, 7) was performed using genes differentially expressed in drug treatment versus normal conditions. These differentially expressed genes were compared to an annotated gene set on Molecular Signatures Database

representing genes that were upregulated in naïve, effector, or memory CD8<sup>+</sup> T cells compared to other CD8<sup>+</sup> T cell populations (Supplemental Information) (8).

#### *SILAC metabolic labeling and sample processing*

To generate labeled CD8<sup>+</sup> T cells with stable isotope-labeled amino acids (Ong et al., 2002), cells were cultured for 72 hours (approximately 6 population doublings) in arginine- and lysine-depleted IMDM media (Cellgro), supplemented at a final concentration of 100 mg/L either with regular 'light' L-Arg and L-Lys (Cambridge Isotopes) or 'heavy' isotope-enriched [U-13C<sub>6</sub>, 15N<sub>2</sub>]-L-Arg and [U-13C<sub>6</sub>, 15N<sub>4</sub>]-L-Lys (Cambridge Isotopes). CD8<sup>+</sup>CD44<sup>hi</sup> cells were sorted and equal cell numbers were mixed 1:1 in the following way for both drug treatments: (1) control labeled / drug unlabeled; (2) control labeled / drug labeled; and (3) (drug unlabeled / control labeled) / (control unlabeled / control labeled). Cell mixtures were lysed with RIPA lysis buffer (50 mM Tris pH 8.5, 150 mM NaCl, 1% Triton-X-100, 0.5% sodium deoxycholate, 0.1% SDS) in the presence of Protease Inhibitor Cocktail (Sigma) and precipitated with methanol and chloroform. 8M urea (in 50 mM ammonium bicarbonate) was added to the protein pellets and extracts were processed with ProteasMAX (Promega) as described by the manufacturer's instructions. The peptides were subsequently reduced with 5 mM Tris(2 carboxyethyl)phosphine at room temperature for 30 min, alkylated in the dark by 10 mM iodoacetamide for 20 min, and digested with Sequencing Grade Modified Trypsin (Promega) overnight at 37°C at an enzyme to sample protein ratio of 1:100, and the reaction was stopped by acidification.

#### *MudPIT and LTA Orbitrap MS analysis*

The peptides were pressure-loaded into a 250- $\mu\text{m}$  i.d. capillary packed with 2.5 cm of 10- $\mu\text{m}$  Jupiter C18 resin (Phenomenex) followed by an additional 2.5 cm of 5- $\mu\text{m}$  Partisphere strong cation exchanger (Whatman). The column was washed for 15 minutes with buffer containing 95% (vol/vol) water, 5% (vol/vol) acetonitrile, and 0.1% formic acid. After washing, a 100- $\mu\text{m}$  i.d capillary with a 5- $\mu\text{m}$  pulled tip packed with 15 cm of 4- $\mu\text{m}$  Jupiter C18 resin was attached to a union, and the entire split column (desalting column–union–analytical column) was placed directly inline with an Agilent 1100 or 1200 quaternary HPLC and analyzed using a modified 11-step separation described previously (2, 9). The data was acquired on a LTQ Orbitrap XL.

#### *Analysis of tandem mass spectra*

Protein identification and quantification and analysis were performed with Integrated Proteomics Pipeline - IP2 (Integrated Proteomics Applications, Inc.) using ProLuCID/Sequest (10), DTASelect2 (11, 12), and Census (13). Mass spectrum raw files were extracted into ms1 and ms2 files from raw files using RawExtract 1.9.9 (14), and the tandem mass spectra were searched against the European Bioinformatic Institute (EBI) mouse protein database. To estimate peptide probabilities and FDRs accurately, we used traditional target/decoy database containing the reversed sequences of all the proteins appended to the target database (15). Tandem mass spectra were matched to sequences using the ProLuCID algorithm done on an Intel Xeon cluster running under the Linux operating system. The search space included all fully and half-tryptic peptide candidates that fell within the mass tolerance window with no miscleavage constraint.

Carbamidomethylation (+57.02146 Da) of cysteine was considered as a static modification. The validity of peptide/spectrum matches (PSMs) was assessed in DTASelect using two SEQUEST-

defined parameters, the cross-correlation score (XCcorr), and normalized difference in cross-correlation scores (DeltaCN). The search results were grouped by charge state (+2, +3, and greater than +3) and tryptic status (fully tryptic, half-tryptic, and nontryptic), resulting in 12 distinct subgroups. In each of these subgroups, the distribution of Xcorr, DeltaCN, and DeltaMass values for (a) direct and (b) decoy database PSMs was obtained; then the direct and decoy subsets were separated by discriminant analysis. Full separation of the direct and decoy PSM subsets is not generally possible; therefore, peptide match probabilities were calculated based on a nonparametric fit of the direct and decoy score distributions. A peptide confidence of 0.95 was set as the minimum threshold. The FDR was calculated as the percentage of reverse decoy PSMs among all the PSMs that passed the confidence threshold. Each protein identified was required to have a minimum of one peptide; however, this peptide had to be an excellent match with an FDR less than 0.001 and at least one excellent peptide match. After this last filtering step, we estimate that both the protein FDRs were below 1% for each sample analysis. Each dataset was searched twice, once against light and then against heavy protein databases. After the results from SEQUEST were filtered using DTASelect2, ion chromatograms were generated using an updated version of Census software (Yates laboratory). Census calculates peptide ion intensity ratios for each pair of extracted ion chromatograms and filters peptide ratio measurements based on a correlation threshold; the correlation coefficient (values between zero and one) represents the quality of the correlation between the unlabeled and labeled chromatograms and can be used to filter out poor-quality measurements. In addition, Census provides an automated method for detecting and removing statistical outliers. The Grubbs test ( $P = 0.01$ ) then is applied to remove outlier peptides. Final protein ratios were generated with QuantCompare, which uses Log fold change and TTest P value to identify regulated significant

proteins. For a protein to be considered in our screen, it had to be “plotted” on our volcano scatter plot. Proteins with peptide counts present in at least three samples,  $p < 0.05$ , and an average ratio of treatment over control greater 1.3 or below -1.3 were considered for analysis.

The y-axis of these volcano plots is the P value, which requires each protein to be quantified in at least two of the biological replicates. Differentially expressed proteins were analyzed using The Database for Annotation, Visualization, and Integrated Discovery (DAVID) to identify Gene Ontology (GO) Biological Function categories that were enriched in each of the drug-treated conditions (16, 17).

#### *Immunofluorescence analysis*

CD8<sup>+</sup> T cells were pre-treated with either DMSO or proteasome activator (cyclosporine) followed by drug washout, then activated for 10 minutes using 10  $\mu\text{g/ml}$  platebound anti-CD3 and CD28, in the presence (‘continuous cyclosporine condition’) or absence of additional cyclosporine (‘cyclosporine pre-treatment and drug washout condition’). Immunofluorescence analysis was performed as previously described (18). The primary antibody used was anti-NFAT1 (D43B1, Cell Signaling). The secondary antibody used was anti-rabbit Alexa Fluor 555 (Life Technologies). DAPI was used to stain DNA (Life Technologies). Images were acquired using a FV1000 laser-scanning confocal microscope (Olympus). Nuclei were distinguished using DAPI staining. The ratio of pixel intensity of nuclear NFAT and total NFAT was quantified in each individual cell using NIH ImageJ software.

#### *Statistics*

Comparison between groups was done using a two-tailed Student's t-test or one-way ANOVA.

P-values < 0.05 were considered significant.

## Supplemental References

1. Banno, A., Garcia, D.A., van Baarsel, E.D., Metz, P.J., Fisch, K., Widjaja, C.E., Kim, S.H., Lopez, J., Chang, A.N., Geurink, P.P., et al. 2016. Downregulation of 26S proteasome catalytic activity promotes epithelial-mesenchymal transition. *Oncotarget*.
2. Florea, B.I., Verdoes, M., Li, N., van der Linden, W.A., Geurink, P.P., van den Elst, H., Hofmann, T., de Ru, A., van Veelen, P.A., Tanaka, K., et al. 2010. Activity-based profiling reveals reactivity of the murine thymoproteasome-specific subunit beta5t. *Chem Biol* 17:795-801.
3. Berkers, C.R., van Leeuwen, F.W., Groothuis, T.A., Peperzak, V., van Tilburg, E.W., Borst, J., Neefjes, J.J., and Ovaa, H. 2007. Profiling proteasome activity in tissue with fluorescent probes. *Mol Pharm* 4:739-748.
4. Chen, J., Bardes, E.E., Aronow, B.J., and Jegga, A.G. 2009. ToppGene Suite for gene list enrichment analysis and candidate gene prioritization. *Nucleic Acids Res* 37:W305-311.
5. Wang, J., Duncan, D., Shi, Z., and Zhang, B. 2013. WEB-based GENE SeT AnaLysis Toolkit (WebGestalt): update 2013. *Nucleic Acids Res* 41:W77-83.
6. Subramanian, A., Tamayo, P., Mootha, V.K., Mukherjee, S., Ebert, B.L., Gillette, M.A., Paulovich, A., Pomeroy, S.L., Golub, T.R., Lander, E.S., et al. 2005. Gene set enrichment analysis: a knowledge-based approach for interpreting genome-wide expression profiles. *Proc Natl Acad Sci U S A* 102:15545-15550.
7. Mootha, V.K., Lindgren, C.M., Eriksson, K.F., Subramanian, A., Sihag, S., Lehar, J., Puigserver, P., Carlsson, E., Ridderstrale, M., Laurila, E., et al. 2003. PGC-1alpha-responsive genes involved in oxidative phosphorylation are coordinately downregulated in human diabetes. *Nat Genet* 34:267-273.
8. Luckey, C.J., Bhattacharya, D., Goldrath, A.W., Weissman, I.L., Benoist, C., and Mathis, D. 2006. Memory T and memory B cells share a transcriptional program of self-renewal with long-term hematopoietic stem cells. *Proc Natl Acad Sci U S A* 103:3304-3309.
9. Washburn, M.P., Wolters, D., and Yates, J.R., 3rd. 2001. Large-scale analysis of the yeast proteome by multidimensional protein identification technology. *Nat Biotechnol* 19:242-247.
10. Lin, W.H., Adams, W.C., Nish, S.A., Chen, Y.H., Yen, B., Rothman, N.J., Kratchmarov, R., Okada, T., Klein, U., and Reiner, S.L. 2015. Asymmetric PI3K Signaling Driving Developmental and Regenerative Cell Fate Bifurcation. *Cell Rep* 13:2203-2218.
11. Verbist, K.C., Guy, C.S., Milasta, S., Liedmann, S., Kaminski, M.M., Wang, R., and Green, D.R. 2016. Metabolic maintenance of cell asymmetry following division in activated T lymphocytes. *Nature* 532:389-393.
12. Pollizzi, K.N., Sun, I.H., Patel, C.H., Lo, Y.C., Oh, M.H., Waickman, A.T., Tam, A.J., Blosser, R.L., Wen, J., Delgoffe, G.M., et al. 2016. Asymmetric inheritance of mTORC1 kinase activity during division dictates CD8(+) T cell differentiation. *Nat Immunol* 17:704-711.
13. Park, S.K., Venable, J.D., Xu, T., and Yates, J.R., 3rd. 2008. A quantitative analysis software tool for mass spectrometry-based proteomics. *Nat Methods* 5:319-322.
14. Tabb, D.L., McDonald, W.H., and Yates, J.R., 3rd. 2002. DTASelect and Contrast: tools for assembling and comparing protein identifications from shotgun proteomics. *J Proteome Res* 1:21-26.

15. McDonald, W.H., Tabb, D.L., Sadygov, R.G., MacCoss, M.J., Venable, J., Graumann, J., Johnson, J.R., Cociorva, D., and Yates, J.R., 3rd. 2004. MS1, MS2, and SQT-three unified, compact, and easily parsed file formats for the storage of shotgun proteomic spectra and identifications. *Rapid Commun Mass Spectrom* 18:2162-2168.
16. Huang da, W., Sherman, B.T., and Lempicki, R.A. 2009. Systematic and integrative analysis of large gene lists using DAVID bioinformatics resources. *Nat Protoc* 4:44-57.
17. Huang da, W., Sherman, B.T., and Lempicki, R.A. 2009. Bioinformatics enrichment tools: paths toward the comprehensive functional analysis of large gene lists. *Nucleic Acids Res* 37:1-13.
18. Chang, J.T., Palanivel, V.R., Kinjyo, I., Schambach, F., Intlekofer, A.M., Banerjee, A., Longworth, S.A., Vinup, K.E., Mrass, P., Oliaro, J., et al. 2007. Asymmetric T lymphocyte division in the initiation of adaptive immune responses. *Science* 315:1687-1691.